

## NEUTRAL-NEUTRAL REACTIONS IN THE INTERSTELLAR MEDIUM. I. FORMATION OF CARBON HYDRIDE RADICALS VIA REACTION OF CARBON ATOMS WITH UNSATURATED HYDROCARBONS

R. I. KAISER,<sup>1</sup> D. STRANGES,<sup>2</sup> Y. T. LEE,<sup>3</sup> AND A. G. SUITS<sup>4</sup>

Received 1996 July 24; accepted 1996 September 23

### ABSTRACT

The reactions of ground-state atomic carbon with acetylene, C<sub>2</sub>H<sub>2</sub> (1), methylacetylene, CH<sub>3</sub>CCH (2), ethylene, C<sub>2</sub>H<sub>4</sub> (3), and propylene, C<sub>3</sub>H<sub>6</sub> (4), are investigated at relative collision energies between 8.8 and 45 kJ mol<sup>-1</sup> in crossed-beam experiments to elucidate the reaction products and chemical dynamics of atom-neutral encounters relevant to the formation of carbon-bearing molecules in the interstellar medium (ISM). Reactive scattering signal is found for C<sub>3</sub>H (1), as well as the hitherto unobserved interstellar radicals C<sub>4</sub>H<sub>3</sub> (2), C<sub>3</sub>H<sub>3</sub> (3), and C<sub>4</sub>H<sub>5</sub> (4). All reactions proceed on the triplet surface via addition of the carbon atom to the molecular  $\pi$ -bond. The initial collision complexes undergo hydrogen migration (1/2) or ring opening (3/4) and decompose via C-H-bond rupture to l/c-C<sub>3</sub>H (1), n-C<sub>4</sub>H<sub>3</sub> (2), propargyl (3), and methylpropargyl (4). The explicit identification of the carbon-hydrogen exchange channel under single collision conditions identifies this class of reaction as a potential pathway to carbon-bearing species in the ISM. Especially, the formation of l/c-C<sub>3</sub>H correlates with actual astronomical observations and explains a higher [c-C<sub>3</sub>H]/[l-C<sub>3</sub>H] ratio in the dark cloud TMC-1 as compared to the carbon star IRC +10216. Our findings strongly demand the incorporation of distinct structural isomers in prospective chemical models of interstellar clouds, hot cores, and circumstellar envelopes around carbon stars.

*Subject headings:* ISM: molecules — methods: laboratory — molecular processes

### 1. INTRODUCTION

Carbon chains and cyclic molecules are common constituents of interstellar clouds, hot cores, and circumstellar envelopes of carbon stars. Hitherto, the homologous series HC<sub>n</sub> ( $n = 1-6$ ), C<sub>n</sub> ( $n = 1, 2, 3, 5$ ), H-(C $\equiv$ C)<sub>n</sub>-CN ( $n = 0-4$ ), (C $\equiv$ C)<sub>n</sub>-CN ( $n = 0, 1$ ), CH<sub>3</sub>-(C $\equiv$ C)<sub>n</sub>-CN ( $n = 0-2$ ), H<sub>2</sub>C<sub>n</sub> ( $n = 3, 4$ ), C<sub>n</sub>O ( $n = 1-3$ ), C<sub>n</sub>S ( $n = 1, 2, 3, 5$ ), and C<sub>n</sub>Si ( $n = 4$ ), as well as the cyclic compounds c-SiC<sub>2</sub>, c-C<sub>3</sub>H<sub>2</sub>, and c-C<sub>3</sub>H have been assigned (Scheffler & Elsässer 1988; Irvine 1992; Cowley 1995). Among them, linear C<sub>3</sub>H, l-C<sub>3</sub>H (propynylidyne), was detected by Thaddeus, Vrtilek, & Gottlieb (1985) via microwave spectroscopy toward the dark Taurus Molecular Cloud 1 (TMC-1) and the carbon star IRC +10216. Two years later, Yamamoto et al. (1987) identified rotational transitions of the cyclic isomer, c-C<sub>3</sub>H (cyclopropynylidyne), in TMC-1 prior to laboratory synthesis (Yamamoto & Saito 1990). Although thermally unstable and extremely reactive in terrestrial laboratories, l/c-C<sub>3</sub>H holds high fractional abundances of  $1.0 \pm 0.7 \times 10^{-9}$  in TMC-1 (Thaddeus et al. 1985), about one order of magnitude less than the ubiquitous cyclopropenylidene, c-C<sub>3</sub>H<sub>2</sub>.

Despite their large interstellar number densities, synthetic routes have not yet been fully resolved. Since the average kinetic energy of interstellar species is confined to typically 0.8 kJ mol<sup>-1</sup> (diffuse clouds) and 0.08 kJ mol<sup>-1</sup> (dark, molecular clouds), gas-phase reactions under thermodynamical equilibrium conditions must have little or no barriers and involve only two body collisions. Ternary

encounters occur only once in a few 10<sup>9</sup> yr and can be neglected considering mean interstellar cloud lifetimes of 10<sup>6</sup> yr. Therefore, chains of radiative association, dissociative recombination, as well as exothermic ion-molecule reactions, have dominated generic chemical models for over two decades (Herbst & Klemperer 1973; Herbst & Delos 1976; Williams 1979; Herbst, Adams, & Smith 1984; Winnewisser & Herbst 1987; Sternberg & Dalgarno 1995; Gerlich & Horning 1992; Smith 1992). The inclusion of exothermic neutral-neutral encounters into chemical models, e.g., of the circumstellar envelope surrounding the carbon star IRC +10216 and the dark cloud TMC-1, occurred only gradually (Graff 1989; Millar, Leung, & Herbst 1990; Herbst & Leung 1990; Clary, Stoecklin, & Wickham 1993; Herbst et al. 1994; Millar & Herbst 1994; Bettens & Herbst 1995; Liao & Herbst 1995; Bettens, Lee, & Herbst 1995), predominantly because entrance barriers were assumed to hinder this reaction class.

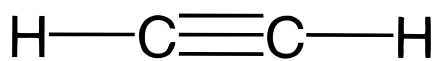
Recently, Husain and co-workers investigated rate constants of C(<sup>3</sup>P<sub>j</sub>) with unsaturated hydrocarbons monitoring the decay kinetics of C(<sup>3</sup>P<sub>j</sub>) at room temperature (Haider & Husain 1993; Husain 1993; Clary et al. 1994). These bulk experiments indicated reactions proceed barrierless and rapidly ( $k = 10^{-10}-10^{-9}$  cm<sup>3</sup> s<sup>-1</sup>) within orbiting limits (Levine & Bernstein 1987). Likewise, kinetic studies of neutral-neutral reactions involving, e.g., OH, CN, and CH radicals at ultralow temperatures revealed rate constants about  $1-6 \times 10^{-10}$  cm<sup>3</sup> s<sup>-1</sup> with maxima between 50–70 K, and only a slight decrease as the temperature falls to 13 K (Sims et al. 1992, 1993, 1994a, 1994b; Canosa et al. 1996). Despite valuable kinetic data, reaction products could not be probed experimentally, and the outcome of neutral-neutral reactions incorporated into interstellar chemical models was predominantly postulated based on spin conservation as well as thermochemistry without investigating distinct structural isomers. This shortcoming clearly

<sup>1</sup> Department of Chemistry, University of California and Chemical Sciences Division, Lawrence Berkeley National Laboratory, Berkeley, CA 94720; kaiser@leea.cchem.berkeley.edu.

<sup>2</sup> Present address: Dipartimento Chimica, Università La Sapienza, Piazzale A. Moro 5, 00185 Rome, Italy; dstranges@axrma.uniroma1.it.

<sup>3</sup> Present address: Academia Sinica, Nankang, Taipei 11529, Taiwan.

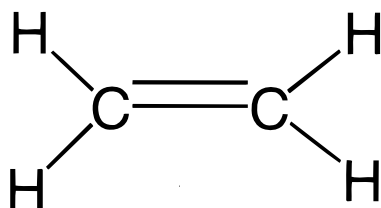
<sup>4</sup> agsuits@lbl.gov.



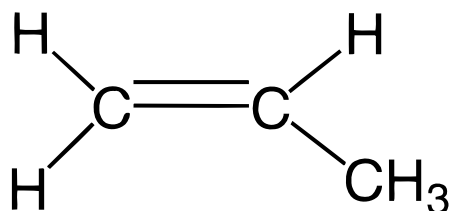
acetylene



methylacetylene



ethylene

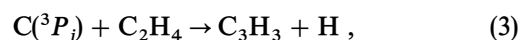
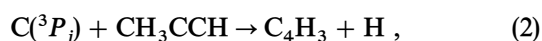
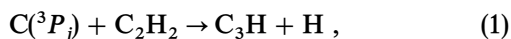


propylene

FIG. 1.—Structure of reactive scattering partners with  $\text{C}({}^3P_j)$ : acetylene (reaction 1), methylacetylene (reaction 2), ethylene (reaction 3), and propylene (reaction 4).

demonstrates the urgency of systematic laboratory examinations to identify the reaction products of neutral-neutral encounters relevant to interstellar chemistry. Since a great variety of structural isomers can contribute to our reactive scattering signal (the simple formula  $\text{C}_4\text{H}_5$  stands for up to 25 distinct isomers), the knowledge of detailed chemical dynamics is crucial to elucidate the product isomer(s).

Here we investigate the following reactions of atomic carbon in its electronic ground state,  $\text{C}({}^3P_j)$ , as a potential source of interstellar carbon hydride radicals (Fig. 1):



Owing to the high reactivity of prospective open shell products, experiments must be performed under single collision conditions to identify the primary reaction products without collisional stabilization or successive reaction of the initially formed complex. Further, hydrocarbon radicals with often unknown spectroscopic properties have to be probed. The requirements are achieved in our studies using the crossed molecular beam technique as described extensively in Lee et al. (1969) and Lee (1988). The reaction channels and selected center-of-mass flux contour plots are presented in § 3 together with results of translational energy distributions and angular distributions in the center-of-mass reference frame. Chemical dynamics and potential energy surfaces (PES) are outlined in § 4. Finally, astrophysical implications are given in § 5.

## 2. EXPERIMENTAL PROCEDURE AND DATA PROCESSING

The universal crossed molecular beam setup and the supersonic carbon source have been described earlier in detail (Lee et al. 1969; Kaiser & Suits 1995). Briefly, the pulsed 266 nm output of a Spectra Physics GCR-270-30 Nd:YAG laser is focused on a rotating carbon rod. Ablated carbon atoms are seeded either into neon or helium carrier gas released by a Prock-Trickl pulsed valve operating at 4 atm backing pressure. A chopper wheel situated after the laser ablation zone selects a  $9.0 \mu\text{s}$  section of the carbon beam. The carbon and the continuous hydrocarbon beam pass through skimmers and cross at  $90^\circ$  in the interaction region. Velocities range from  $1100$  to  $3200 \text{ ms}^{-1}$  (carbon beam) and  $780$ – $870 \text{ ms}^{-1}$  (hydrocarbon beam) with speed ratios of  $2.6$ – $6.0$  and  $7.0$ – $9.3$ , respectively. Reactively scattered products are monitored in the collision plane using a triply differentially pumped quadrupole mass spectrometer with a Brink-type electron-impact ionizer in the time-of-flight (TOF) mode, i.e., recording the time-dependent intensity of ions at one  $m/e$ -ratio at different laboratory scattering angles.

Information on the reaction dynamics is gained by fitting the TOF spectra and the product angular distribution LAB in the laboratory reference frame using a forward-convolution routine (Vernon 1981; Weiss 1986). This iterative approach initially guesses the angular flux distribution  $T(\theta)$  and the translational energy flux distribution  $P(E_T)$  in the center-of-mass system (CM) which are assumed to be independent of each other. Laboratory TOF spectra and LAB distribution are calculated from these  $T(\theta)$  and  $P(E_T)$  averaged over a grid of Newton diagrams and the apparatus functions, and best TOF and laboratory angular distributions achieved by iteratively refining adjustable  $T(\theta)$  and  $P(E_T)$  parameters. Finally, a center-of-mass flux contour map  $I(\theta, E_T) \sim T(\theta)P(E_T)$ , which contains all the dynamical information of the reactive scattering process, is computed.

## 3. RESULTS

### 3.1. Reactive Scattering Signal

The carbon-hydrogen exchange channels (1)–(4) dominate the product distributions, and reactive scattering signal is only observed at  $m/e = 37, 51, 39,$  and  $53$ , i.e.,  $\text{C}_3\text{H}$  (reaction 1),  $\text{C}_4\text{H}_3$  (reaction 2),  $\text{C}_3\text{H}_3$  (reaction 3), and  $\text{C}_4\text{H}_5$

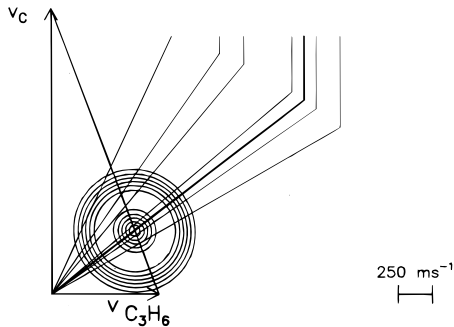
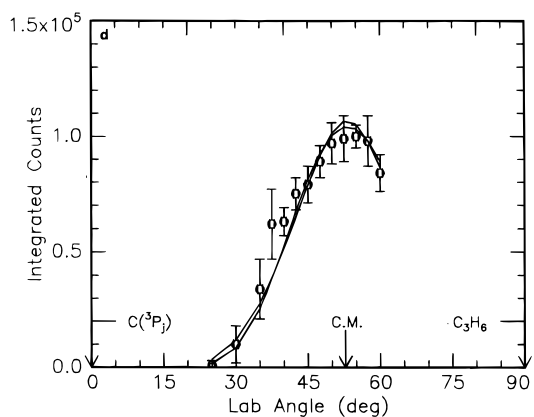
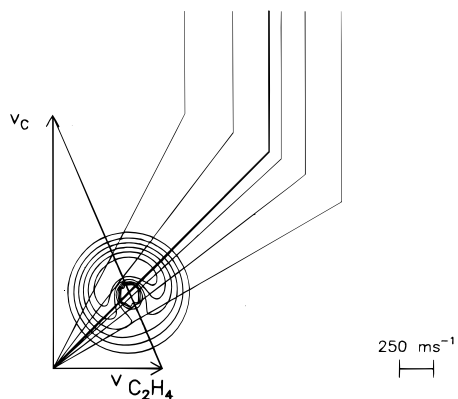
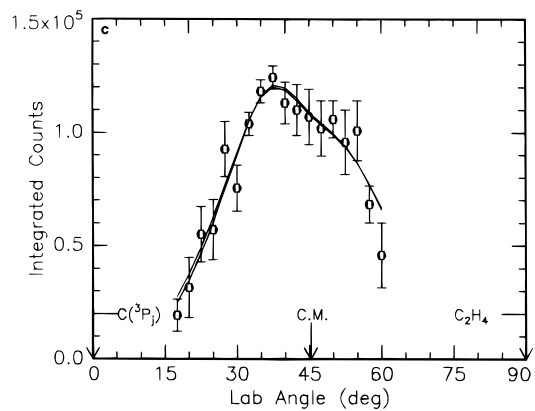
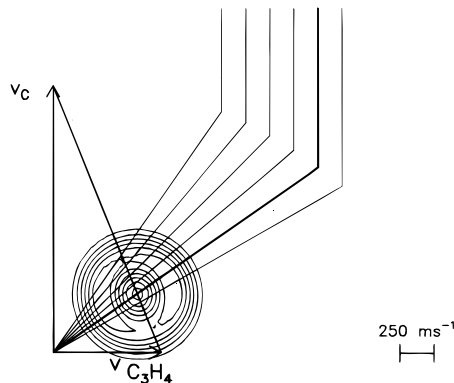
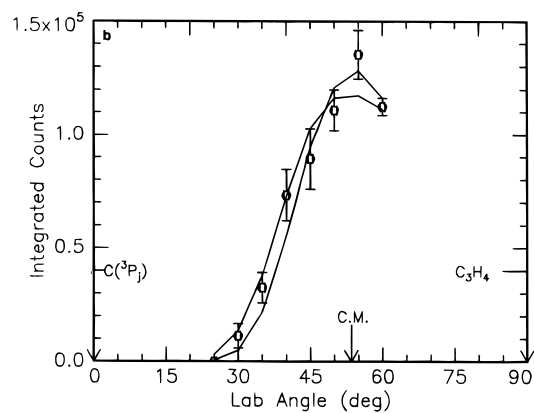
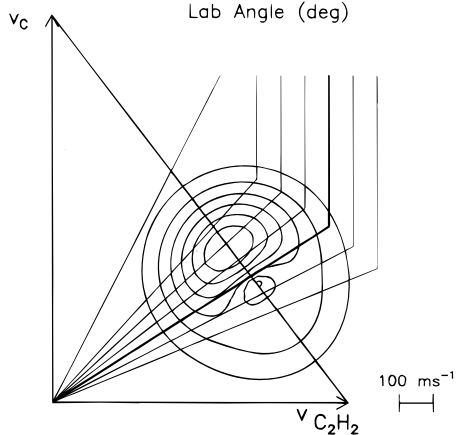
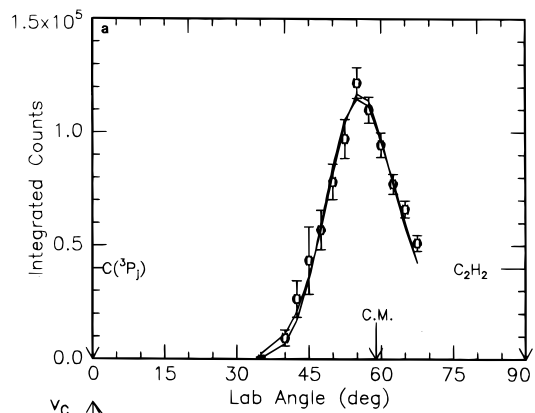


FIG. 2.—*Top*: Laboratory angular distributions of (a)  $C_3H$ , (b)  $C_4H_3$ , (c)  $C_3H_3$  and (d)  $C_4H_5$  at collision energies of 8.8, 20.4, 17.1, and 23.3  $\text{kJ mol}^{-1}$ , respectively. Open circles represent measured data within  $1\sigma$  error bars, the solid lines the calculated distributions. *Bottom*: Most probable Newton diagrams and flux contour maps of (1)–(4) at collision energies of (a) 8.8, (b) 20.4, (c) 17.1 and (d) 23.3  $\text{kJ mol}^{-1}$ .

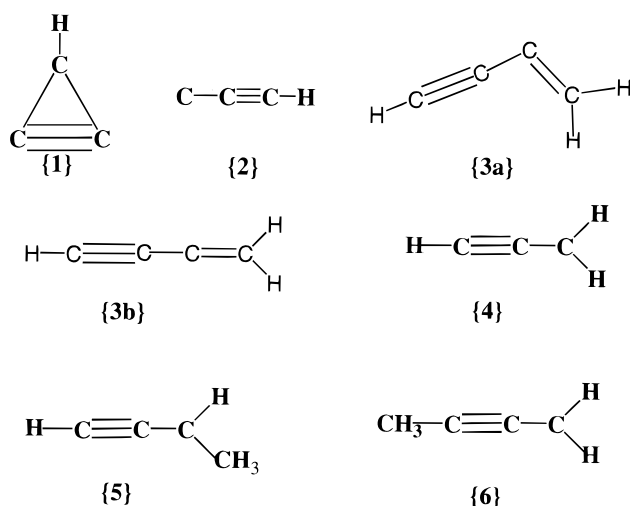


FIG. 3.—Reactive scattering products of reactions (1)–(4): cyclopropynylidyne ( $c\text{-C}_3\text{H}$  {1}), propynylidyne ( $l\text{-C}_3\text{H}$  {2}),  $\alpha$ -ethynylvinyl/butatrienyl ( $n\text{-C}_4\text{H}_3$  {3a}/{3b}), propargyl ( $l\text{-C}_3\text{H}_3$  {4}), and 1- or 3-methylpropargyl ( $l\text{-C}_4\text{H}_5$  {5}/{6}). The equilibrium geometry of bent {3a} vs. linear  $n\text{-C}_4\text{H}_3$  {3b} has not yet been resolved (Kasai, Skattebol, & Whipple 1986; Kasai 1972; Cooky 1995).

(reaction 4). The observation of these reaction channels under single collision conditions alone underlines the potential importance of this reaction class to build up carbon-bearing molecules in interstellar environments. TOF spectra recorded at lower  $m/e$  values 36 (reaction 1), 48–50 (reaction 2), 36–38 (reaction 3), and 48–52 (reaction 4) show identical patterns indicating the signal originates in cracking of the parent in the ionizer. In addition, no radiative associations to  $\text{C}_3\text{H}_2$ ,  $\text{C}_4\text{H}_4$ ,  $\text{C}_3\text{H}_4$ , and  $\text{C}_4\text{H}_6$  or higher masses are observed. This result strongly demonstrates that the highly internally excited and initially formed adducts do not survive under single collision conditions in our experiments as well as in the ISM; however, denser planetary or cometary atmospheres can supply a third body reaction to stabilize these intermediates.

### 3.2. Laboratory Angular Distributions

Figure 2 displays the laboratory angular distributions (LAB) of  $\text{C}_3\text{H}$  (1),  $\text{C}_4\text{H}_3$  (2),  $\text{C}_3\text{H}_3$  (3), and  $\text{C}_4\text{H}_5$  (4) at selected collision energies  $E_{\text{coll}}$  of 8.8 (1), 20.4 (2), 17.1 (3), and 23.3  $\text{kJ mol}^{-1}$  (4) together with the most probable Newton diagrams and flux contour maps. Comparison of the reactive scattering range of these distributions with limit circles of different structural isomers confines energetically accessible  $\text{C}_3\text{H}_3$  products to the propargyl, cyclopropen-yl, or propyn-yl isomer. The explicit limitation to distinct  $\text{C}_3\text{H}$ ,  $\text{C}_4\text{H}_3$ , and  $\text{C}_4\text{H}_5$  isomers solely based on limit circles is not possible, since individual circles are blurred out due to the velocity spread of the carbon beam (§ 2).

### 3.3. Center-of-Mass Translational Energy Distributions, $P(E_T)$

Best fits of TOF spectra and LAB distributions are achieved with  $P(E_T)$  values extending to a maximum translational energy, i.e., the sum of the reaction exothermicity and relative collision energy, of  $E_{\text{max}} = 30\text{--}90$   $\text{kJ mol}^{-1}$  (1), 230–255  $\text{kJ mol}^{-1}$  (2), 225–255  $\text{kJ mol}^{-1}$  (3), and 210–230  $\text{kJ mol}^{-1}$  (4). The order of magnitude of this high-energy cutoff can be employed to identify the product isomer if their energetics are well separated. Within the error limits,

data are consistent with the formation of  $n\text{-C}_4\text{H}_3$  {3a}/{3b} (reaction 2; Kaiser et al. 1996c), the propargyl radical  $\text{C}_3\text{H}_3$  {4} (reaction 3; Kaiser, Lee, & Suits 1996a), and the 1- and/or 3-methylpropargyl radical {5}/{6} (reaction 4; Kaiser et al. 1996d), Figure 3. The linear {2} and cyclic  $\text{C}_3\text{H}$  {1} isomers cannot be separated based solely on the  $P(E_T)$  values since both enthalpies of formations differ only by about 7.5  $\text{kJ mol}^{-1}$  (Ochsenfeld et al. 1996).

### 3.4. Center-of-Mass Angular Distributions, $T(\theta)$

#### 3.4.1. Reaction $\text{C} + \text{C}_2\text{H}_2$ (1)

As the collision energy increases, the center-of-mass angular distributions change significantly and exhibit decreasing intensity ratios at the poles from  $I(0^\circ)/I(180^\circ) = 2.6$  via 1.2 to 1.0. These data show the disappearance of forward-peaked products with respect to the carbon beam at higher collision energies and suggest decomposing the single angular distribution into two distinct micromechanisms, an isotropic channel at all collision energies (No. 1) and a second, forward-peaked contribution at 8.8 and 28.7  $\text{kJ mol}^{-1}$ . The asymmetric  $T(\theta)$  of microchannel 2 implies a decomposing  $\text{C}_3\text{H}_2$  complex in which both hydrogen atoms cannot be converted via a rotation axis or mirror plane. Microchannel 1 involves either a symmetric  $\text{C}_3\text{H}_2$  structure (interconversion of both H atoms via rotation axis or mirror plane) or passes through a deep potential well with a lifetime of the fragmenting complex longer than its rotational period.

#### 3.4.2. Reactions $\text{C} + \text{CH}_3\text{CCH}$ (2) and $\text{C} + \text{C}_3\text{H}_6$ (4)

At lower collision energies,  $T(\theta)$  values of (2) and (4) are symmetric around  $\pi/2$ , implying that either the fragmenting  $\text{C}_4\text{H}_4/\text{C}_4\text{H}_6$  complex holds a lifetime longer than the rotational period or that it is symmetric. With increasing collision energy, the shapes of both distributions change significantly and depict a rising intensity at  $0^\circ$ . These findings suggest a reduced lifetime of the decomposing complexes as the collision energy rises and eliminate symmetric  $\text{C}_4\text{H}_4$  as well as  $\text{C}_4\text{H}_6$  complexes.

#### 3.4.3. Reaction $\text{C} + \text{C}_2\text{H}_4$ (3)

Both  $T(\theta)$  values show a decreasing fraction of forward-peaking reactive scattering signal with rising collision energy. These data indicate the reaction proceeds via two microchannels, the first one isotropic, and the second channel forward scattered with respect to the carbon beam. Further, the decomposing  $\text{C}_3\text{H}_4$  complex has to be asymmetric.

## 4. CHEMICAL DYNAMICS

In the following section, we outline the chemical dynamics of reactions (1)–(4) and discuss involved PESs via initial addition of the carbon atom to the hydrocarbon reactant. Insertion into carbon-hydrogen (reactions [1]–[4]) and carbon-carbon single bonds (reactions [2] and [4]) as well as intersystem crossing (ISC) to the singlet surface do not contribute to the reactive scattering signal, since the expected chemical dynamics of both processes do not correlate with the experimentally observed center-of-mass angular and translational energy distributions (Kaiser et al. 1996a, 1996b, 1996c, 1996d). A analysis of the chemical dynamics is essential to reveal information on the product isomers formed in reactions (1)–(4). Since our laboratory data strongly depend on the structure(s) of the fragmenting

complex(es) to the reaction products, we first investigate the geometries of energetically accessible collision complexes. We then compare our crossed-beam data and experimental dynamics with those arising from distinct adducts. Once the isomer(s) is (are) identified, we ultimately reveal the product channel(s).

#### 4.1. Reaction $C + C_2H_2$ (1)

Figure 4 displays a schematic energy diagram of the triplet  $C_3H_2$  PES and feasible exit channels to  $1/c-C_3H$ . First, we elucidate the isomer leading to the isotropic microchannel. An interpretation of a long-lived  $C_3H_2$  collision complex contributing to an isotropic  $T(\theta)$  can be eliminated, since the energy well depth even of the energetically most favorable propargylene is expected to be less than the rotation period of the reaction intermediate. The evidence is even stronger if we compare the dynamics with those of the reaction  $C(^3P) + CH_3CCH(X^1A_1)$  (Kaiser et al. 1996c). Therefore, microchannel one originates in a symmetric  $C_3H_2$  isomer, i.e.,  $H_2CCC$  or  $HCCCH$ , since a rotation around the  $C_2$  rotation axis interconverts both H atoms. However, if  $H_2CCC$  was formed, the fragmenting complex would rotate around the  $C_2$  symmetry axis to yield exclusively  $1-C_3H(X^2\Pi_j)$ . This linear isomer would be excited to rotations around its internuclear axis, but due to the vanishing moment of inertia this rotation is not energetically accessible, and this pathway cannot account for rotational excitation in  $1-C_3H$ . These findings reveal that this symmetric channel must originate in the rotation of  $HCCCH$  around the  $C_2$  axis fragmenting to  $C_3H(X^2\Pi_j)$  and a hydrogen atom. The  $HCCCH$  complex itself is formed via an initial addition of atomic carbon to acetylene to form

triplet propenediylidene {7} followed by hydrogen migration to propargylene.

The second microchannel arises from an initially formed triplet  $c-C_3H_2$  collision complex decomposing to  $c-C_3H$  and atomic hydrogen (Kaiser et al. 1996b). The large deviation of the relative cross sections from the classical capture theory resolves the underlying dynamics for this microchannel. Although the detailed structure of the molecule does not play a role within the simple capture framework, this approximation breaks down as the orbiting radius decreases with rising collision energy: reactive encounters from radii exceeding the symmetric  $\pi$ -cloud to form  $c-C_3H_2$  become more and more unlikely and are preferentially shifted toward orbits in which the  $\pi$ -cloud can be attacked sideways to yield the CCHCH isomer. This model explains both the decreasing cross section and less polarized center-of-mass angular distribution as the collision energy rises.

Recent ab initio investigations of reaction (1) by Takahashi & Yamashita (1996) report the reaction to both  $C_3H$  isomers is slightly endothermic. Further, they concluded only the cyclic  $C_3H$  isomer is formed. This study, however, shows only a limited treatment of the triplet  $C_3H_2$  surface. The initial addition step is restricted to only one  $C_3H_2$  isomer (propenediylidene) and does not consider the direct formation of triplet  $c-C_3H_2$ . Further, no hydrogen migration in the initial addition complex is discussed. Most important, however, Takahashi & Yamashita employ an unstable wave function to calculate the geometry of the propenediylidene isomer. Since this structure represents the key to their conclusions, and intersystem crossing from the triplet to singlet surface and back to the triplet one is purely speculative, this paper cannot give a conclusion to the reac-

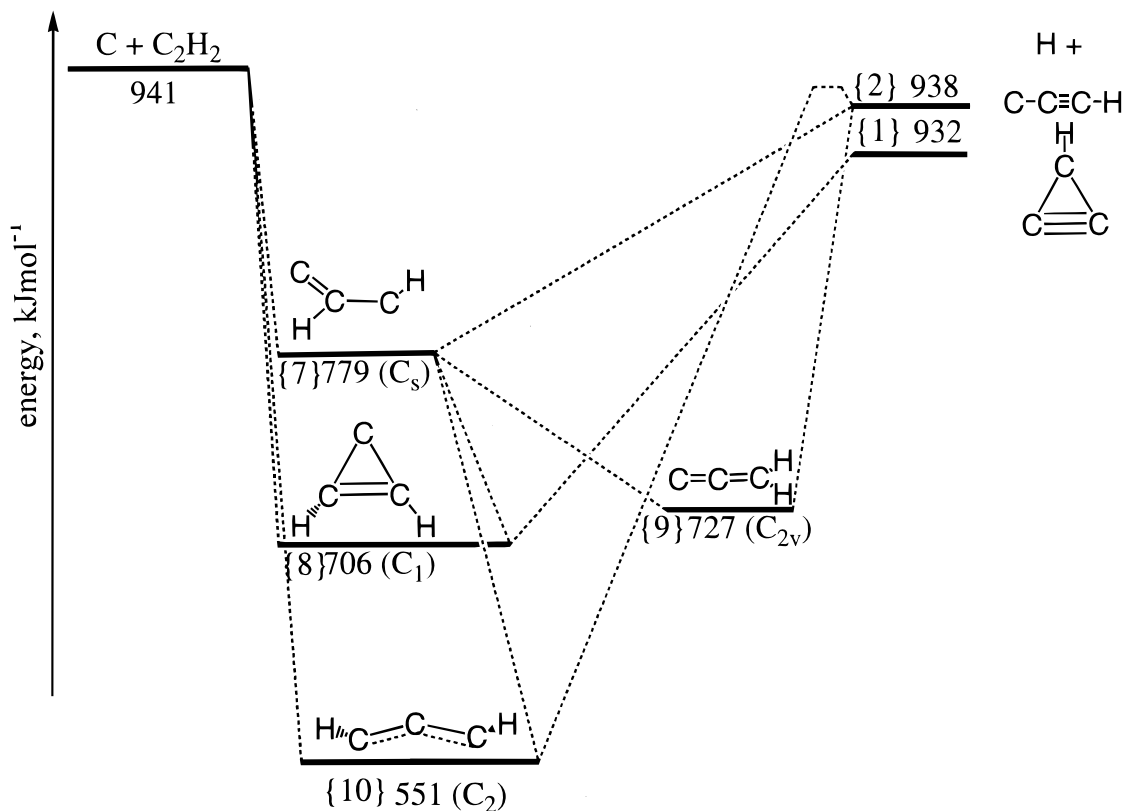
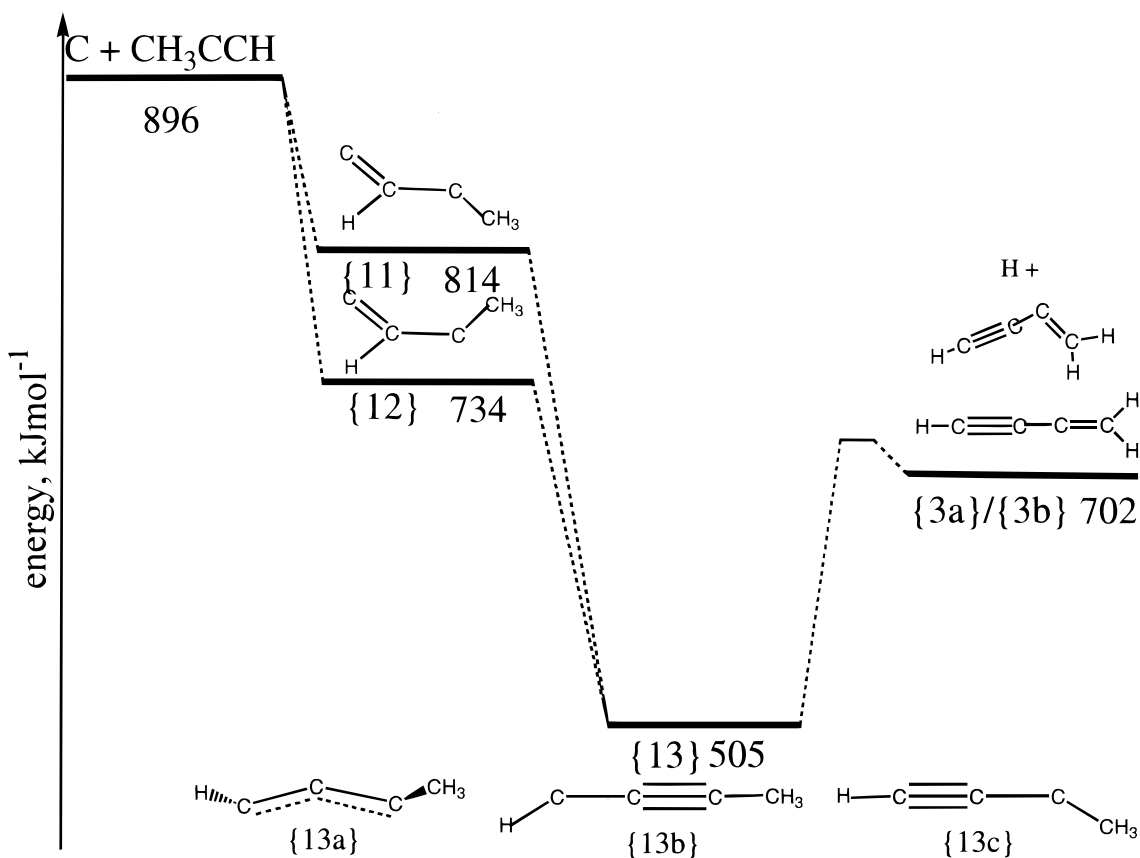


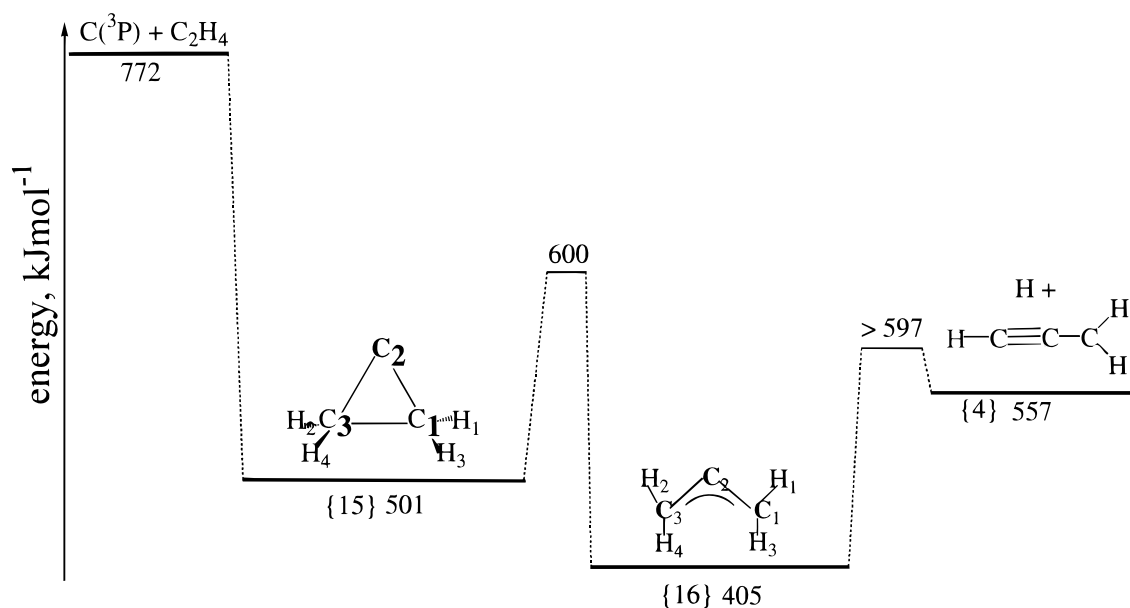
FIG. 4.—Schematic potential energy diagram of the triplet  $C_3H_2$  PES. Enthalpies of formation in  $\text{kJ mol}^{-1}$  and point groups are compiled in Kaiser et al. (1996b).

FIG. 5.—Schematic potential energy diagram of the triplet  $\text{C}_4\text{H}_4$  PES

tion products of (1). Finally, we would like to point out that very recent ab initio calculations on the global triplet  $\text{C}_3\text{H}_2$  surface on a higher level of theory show indeed that the reaction to l- as well as c- $\text{C}_3\text{H} + \text{H}$  is exothermic by 1.3 and 8.6  $\text{kJ mol}^{-1}$  as found in our experiments (Ochsenfeld et al. 1996).

#### 4.2. Reaction $\text{C} + \text{CH}_3\text{CCH}$ (2)

Conserving the C-C-C-C plane as a symmetry element, occupied  $\text{C}(^3P_j)$  adds to the  $\beta$ -C-atom of methylacetylene to form triplet 1-methylpropendiylidene  $\{11\}/\{12\}$  (see Fig. 5) (Kaiser et al. 1996c) similar to the reaction (1). A consecu-

FIG. 6.—Schematic potential energy diagram of the triplet  $\text{C}_3\text{H}_4$  PES (Kaiser et al. 1996d). Enthalpies of formation are in  $\text{kJ mol}^{-1}$ .

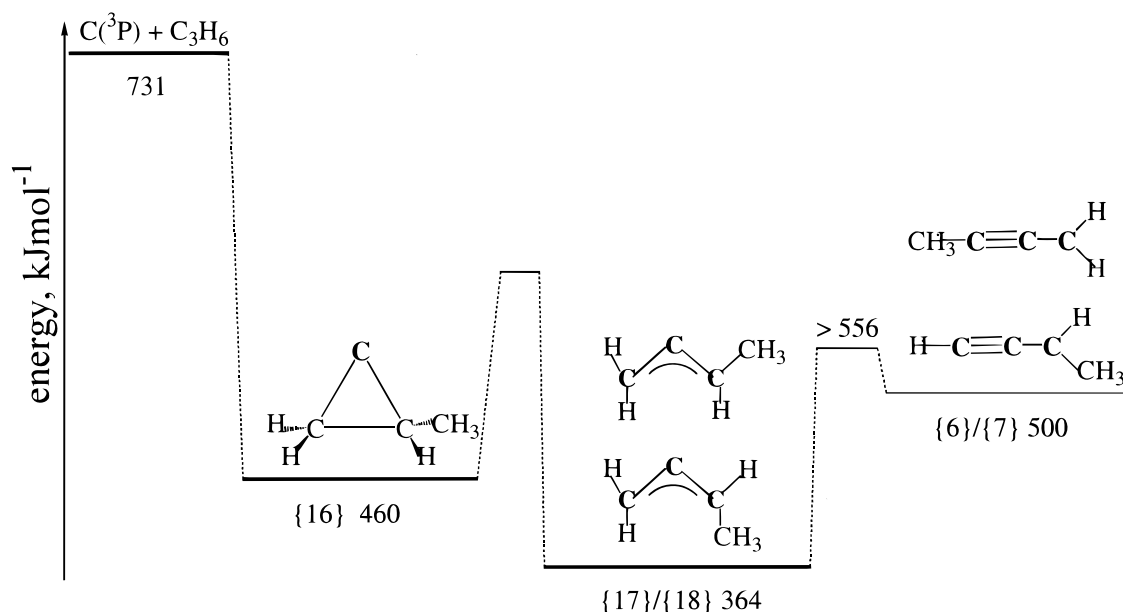


FIG. 7.—Schematic potential energy diagram of the triplet  $C_4H_6$  PES modified from Kaiser et al. 1996c

tive hydrogen shift forms triplet 1-methylpropargylene {13} decomposing via C-H bond rupture to  $n-C_4H_3$  and H.

#### 4.3. Reaction $C + C_2H_4$ (3)

$C(^3P_j)$  adds to the  $C_2H_4$  double bond on the triplet surface (Kaiser et al. 1996b) (see Fig. 6). The successive ring opening to triplet allene {16} converts the previously out-of-plane H atoms into the symmetry plane. Finally, C-H bond cleavage yields the propargyl radical and atomic hydrogen. A dominating in-plane rotation of the  $C_4H_3$  complex yields extremely low  $K$  value and can be related to preferentially low  $K$  states populated in the propargyl radical. The forward scattered microchannel 2 arises from C-like rotations of the triplet allene complex.

#### 4.4. Reaction $C + C_3H_6$ (4)

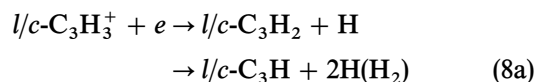
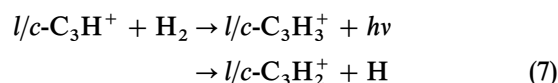
Similarly to reaction (3), atomic carbon adds to the olefinic double bond to form methyl-cyclopropylidene (see Fig. 7) which undergoes ring opening to triplet 1,2 butadiene {17/18}. The H1 loss yields the 1-methylpropargyl radical, whereas C3-H2/C3-H3 bond rupture forms 3-methylpropargyl. Both isomers differ by only  $3 \text{ kJ mol}^{-1}$  and cannot be distinguished based on our present experimental data.

### 5. ASTROPHYSICAL IMPLICATIONS

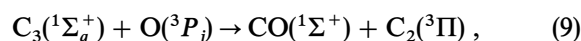
The crossed molecular beam technique has been proven a powerful tool to investigate neutral-neutral reactions of potential importance to interstellar chemistry. Besides identification of distinct product isomers, information on chemical dynamics and involved collision complexes are also supplied. The chemical dynamics that cause an increasing ratio of  $l-C_3H$  to  $c-C_3H$  with rising collision energy explain previously unresolved astronomical observations. Dark molecular clouds hold typical averaged translational temperatures of 10 K, whereas circumstellar shells around carbon stars are heated up to about 4000 K giving mean translational energies of about 0.1 and  $40 \text{ kJ mol}^{-1}$ , respectively. Therefore, both isomers are anticipated to exist in dark clouds, but less  $c-C_3H$  in the hotter envelope sur-

rounding IRC + 10216. This expected pattern is reflected in observed number density ratios of  $c-C_3H$  versus  $l-C_3H$  of unity in cold molecular clouds, e.g., TMC-1, versus  $0.2 \pm 0.1$  around IRC + 10216. Therefore, a common acetylene reactant to interstellar  $l/c-C_3H$  radicals via atom-neutral reaction with  $C(^3P_j)$  and distinct structural isomers must be included into interstellar reaction networks.

Most important, the explicit identification of the carbon-hydrogen exchange channel to  $l/c-C_3H$ ,  $n-C_4H_3$ , propargyl, and methylpropargyl radicals under single collision conditions represents an alternative pathway to competing ion-molecule reactions. The ionization of neutral carbon atoms (5), for example, initiates a four-step mechanism to  $C_3H$  via ion-molecule reaction of singly ionized carbon with acetylene (6) followed by radiative association (7) and dissociative recombination (8). This sequence is in contrast to a single C- $C_2H_2$  encounter forming  $C_3H$  (1):



The actual contribution of carbon-unsaturated hydrocarbon reactions to complex species in interstellar environments depends strongly on the imposed synthetic chemical reaction network and minor entrance barriers to the PES. Based on the molecular cloud model of Millar et al. (1987) and Bettens et al. (1995), reactions of N as well as O atoms are thought to be rate limiting and destroy produced complex molecules. Very recent rate calculations of (9), however,



do not support this conclusion—at least for the  $C_3$  carbon cluster—since an entrance barrier of  $7.5 \text{ kJ mol}^{-1}$  inhibits this reaction in warm as well as cold interstellar clouds (Woon & Herbst 1996). Unlike this scenario, inclusion of C atom reactions in a model of the circumstellar envelope surrounding the carbon star IRC + 10216 does not lead to a destruction of complex, carbon-bearing species since the ratio of atomic carbon to oxygen is greater than unity. Further, lowest investigated collision energies of  $8.8 \text{ kJ mol}^{-1}$  in our experiments are equivalent to about 900 K versus a maximum translational temperature of ca. 100 K in molecular clouds, but up to 4000 K in outflow of carbon stars. Although our data depict rising reaction cross sections as the collision energy falls (Kaiser et al. 1996a, 1996c, 1996d), extrapolation to interstellar temperatures as low as 10–100 K depends on the absence of even small barriers. A strong interplay of crossed beam experiments and low-temperature kinetic studies is desirable.

Our findings should encourage an actual search for the hitherto unobserved radicals  $l\text{-C}_3\text{H}_3$ ,  $n\text{-C}_4\text{H}_3$ , and  $C_4\text{H}_5$ . In particular, methylacetylene has been widely observed toward, e.g., the Orion Ridge, Sagittarius B2, and TMC-1 (Gerin et al. 1992). These clouds serve as ideal targets to identify potential  $C_4\text{H}_3$ -isomers, perhaps in unidentified microwave transitions in the spectrum toward the extended ridge of OMC-1 (Sutton et al. 1995).

R. I. K. is indebted to the Deutsche Forschungsgemeinschaft for a postdoctoral fellowship and to the IAU for financial support to present these results on the IAU Symp. 178, *Molecules in Astrophysics: Probes and Processes*, in Leiden, The Netherlands. This work was further supported by the Director, Office of Energy Research, Office of Basic Energy Sciences, Chemical Sciences Division of the US Department of Energy under contract No. DE-AC03-76SF00098.

## REFERENCES

- Bettens, R. P. A., & Herbst, E. 1995, *Int. J. Mass Spectrom. Ion. Phys.*, 149/150, 321
- Bettens, R. P. A., Lee, H. H., & Herbst, E. 1995, *ApJ*, 443, 664
- Canosa, A., Sims, I. R., Travers, D., Smith, I. W. M., & Rowe, B. R. 1996, *A&A*, submitted
- Clary, D. C., Haider, N., Husain, D., & Kabir, M. 1994, *ApJ*, 422, 416
- Clary, D. C., Stoecklin, T. S., & Wickham, A. G. 1993, *J. Chem. Soc. Faraday Trans.*, 89, 2185
- Cooksy, A. L. 1995, *J. Am. Chem. Soc.*, 117, 1098
- Cowley, C. R. 1995, *An Introduction to Cosmochemistry* (Cambridge: Cambridge Univ. Press)
- Gerin, M., Combes, F., Wlodarczak, G., Encrenaz, P., & Laurent, C. 1992, *A&A*, 253, 29
- Gerlich, D., & Horning, S. 1992, *Chem. Rev.*, 92, 1509
- Graff, M. M. 1989, *ApJ*, 339, 239
- Haider, N., & Husain, D. 1993, *J. Photochem. Photobiol.*, A70, 119
- Herbst, E., Adams, N. G., & Smith, D. 1984, *ApJ*, 285, 618
- Herbst, E., & Delos, J. 1976, *Chem. Phys. Lett.*, 42, 54
- Herbst, E., & Klemperer, W. 1973, *ApJ*, 185, 505
- Herbst, E., Lee, H. H., Howe, D. A., & Millar, T. J. 1994, *MNRAS*, 268, 335
- Herbst, E., & Leung, C. M. 1990, *ApJ*, 233, 170
- Husain, D. 1993, *J. Chem. Soc. Faraday Trans.*, 89, 2164
- Irvine, W. M. 1992, presented at COSPAR, Washington D.C.
- Kaiser, R. I., Lee, Y. T., & Suits, A. G. 1996a, *J. Chem. Phys.*, to be submitted
- , 1996b, *J. Chem. Phys.*, in press
- Kaiser, R. I., Stranges, D., Lee, Y. T., & Suits, A. G. 1996c, *J. Chem. Phys.*, in press
- , 1996d, *J. Chem. Phys.*, submitted
- Kaiser, R. I., & Suits, A. G. 1995, *Rev. Sci. Instr.*, 66, 5405
- Kasai, P. H. 1972, *J. Am. Chem. Soc.*, 94, 5950
- Kasai, P. H., Skattemol, L., & Whipple, E. B. 1986, *J. Am. Chem. Soc.*, 90, 4509
- Lee, Y. T. 1988, in *Atomic and Molecular Beam Methods*, Vol. 1, ed. G. Scoles (Oxford: Oxford Univ. Press), 553
- Lee, Y. T., McDonald, J. D., LeBreton, P. R., & Herschbach, D. R. 1969, *Rev. Sci. Instr.*, 40, 1402
- Levine, R. D., & Bernstein, R. B. 1987, *Molecular Reaction Dynamics and Chemical Reactivity* (Oxford: Oxford Univ. Press)
- Liao, Q., & Herbst, E. 1995, *ApJ*, 444, 694
- Millar, T. J., & Herbst, E. 1994, *A&A*, 288, 561
- Millar, T. J., Leung, C. N., & Herbst, E. 1987, *A&A*, 183, 109
- Ochsenfeld, C., Kaiser, R. I., Lee, Y. T., Suits, A. G., & Head-Gordon, M. 1996, *J. Chem. Phys.*, submitted
- Scheffler, H., & Elsässer, H. 1988, *Physics of the Galaxy and Interstellar Matter* (Berlin: Springer)
- Sims, I. R., Queffelec, J., Defrance, A., Rebrion-Rowe, C., Travers, D., Bocherel, P., Rowe, B. R., & Smith, I. W. M. 1994a, *J. Chem. Phys.*, 100, 4229
- Sims, I. R., Queffelec, J., Defrance, A., Rebrion-Rowe, C., Travers, D., Rowe, B. R., & Smith, I. W. M. 1992, *J. Chem. Phys.*, 97, 8798
- Sims, I. R., Queffelec, J., Travers, D., Bocherel, P., Rowe, B. R., Herbert, L. B., Karthaus, J., & Smith, I. W. M. 1993, *Chem. Phys. Lett.*, 211, 461
- Sims, I. R., Smith, I. W. M., Bocherel, P., Defrance, A., Travers, D., & Rowe, B. R. 1994b, *J. Chem. Soc. Faraday Trans.*, 90, 1473
- Smith, D. 1992, *Chem. Rev.*, 92, 1580
- Sternberg, A., & Dalgarno, A. 1995, *ApJS*, 99, 565
- Sutton, E. C., Peng, R., Danchi, W. C., Jaminet, P. A., Sandell, G., & Russel, A. P. G. 1995, *ApJS*, 97, 455
- Takahashi, J., & Yamashita, K. 1996, *J. Chem. Phys.*, 104, 6613
- Thaddeus, P., Vrtilik, J. M., & Gottlieb, C. A. 1985, *ApJ*, 299, L63
- Vernon, M. 1981, LBL Rep. 12422
- Weiss, M. S. 1986, Ph.D. thesis, Univ. California, Berkeley
- Woon, D. E., & Herbst, E. 1996, *ApJ*, 465, 795
- Williams, D. A. 1979, *Astrophys. Lett.*, 10, 17
- Winniewisser, G., & Herbst, E. 1987, in *Topics in Current Chemistry*, 139, 121
- Yamamoto, S., & Saito, S. 1990, *ApJ*, 363, L13
- Yamamoto, S., Saito, S., Ohishi, M., Suzuki, H., Ishikawa, S. I., Kaifu, H., & Murakami, A. 1987, *ApJ*, 322, L55